LithoMamba: High-fidelity lithography simulation with State Space Models

Xinyu He[1,2,3], Daohui Wang[1,2], Shujing Lyu[1,2], Pourya Shamsolmoali[1,2], Jiwei Shen[1,2], Yue Lu[1,2]
[1]Shanghai Key Laboratory of Multidimensional Information Processing, East China Normal University, China
[2]School of Communication and Electronic Engineering, East China Normal University, China
[3]Shanghai Innovation Institution, China
hexinyu@stu.ecnu.edu.cn, ylu@cee.ecnu.edu.cn

***Abstract*—Lithography simulation is a critical technology in modern semiconductor manufacturing, yet existing deep learning models often fail to accurately model the complex, long-range optical physics due to the inherent locality of convolution. This limitation results in insufficient simulation fidelity and poses significant challenges for optimization tasks. To overcome this challenge, we introduce LithoMamba, the first generative framework to leverage Mamba for high-fidelity lithography simulation. Our architecture uses a Mamba Generator to model global and long-range optical interactions, while a local, MLP-free Discriminator provides precise, spatial feedback to ensure fine-grained pattern fidelity. This global-local design enables our model to achieve both physical realism and exceptional detail. Our experiments show that LithoMamba outperforms existing methods, both in quantitative and qualitative results. These findings demonstrate the promise of State Space Models for improving lithography simulation and suggest new possibilities for combining physics with generative AI in chip manufacturing.**

***Index Terms*—Lithography Simulation, Mamba, GAN, Image Generation**

I. Introduction

Lithography simulation is a key technology in modern semiconductor manufacturing. It plays a critical role in improving yield and IC performance through applications such as optical proximity correction and source-mask optimization [1], [2]. In recent years, deep generative models, particularly convolution-based Generative Adversarial Networks (GANs), have emerged as a promising approach for this task, translating IC layout designs into corresponding Scanning Electron Microscope (SEM) images [3]–[8]. However, the efficacy of these methods is fundamentally constrained by the local receptive fields of convolution. This inherent locality struggles to accurately model the long-range interactions of optical physics like diffraction [9], [10], yielding abnormal and blurry results. While recent approaches incorporate Fourier transforms to capture global information, they often sacrifice high-frequency spatial details, which are crucial for pattern fidelity [11], [12].

Recent advancements in State Space Models (SSMs), particularly Mamba, have demonstrated remarkable capabilities in modeling long-range dependencies with computational efficiency [13]–[15]. In this work, we introduce LithoMamba, a novel generative framework specifically designed for high-fidelity lithography simulation. Our framework uniquely combines the strengths of SSMs for global modeling and localized adversarial feedback for fine detail synthesis.

The proposed Mamba Generator is built upon the Mamba architecture [13]. By processing the input IC layout as a sequential scan, the generator leverages mamba to inherent its global modeling capability. This design enables it to explicitly model the complex, long-range optical effects fundamental to the lithography process [9], progressively encoding the layout and reconstructing the SEM image. To complement this global generator, we propose a Local Discriminator. Inspired by the translational invariance of IC patterns, our discriminator, based upon convolution, is designed to produce a localized adversarial score map by forgoing the final global aggregation layer. Each element in this map provides a spatially-aware feedback signal, guiding the generator to focus on intricate, local patterns. This joint global-local architecture creates a powerful synergy: the generator models the overarching physics, while the localized feedback from the discriminator refines the details. Our main contributions are summarized as follows:

- We propose LithoMamba, the first framework to leverage a State Space Model (Mamba) for the task of lithography simulation, demonstrating its suitability for modeling complex physical processes in semiconductor manufacturing.
- We introduce a novel global-local generative architecture. The Mamba Generator effectively captures long-range optical effects, while our Local Discriminator, exploiting the translational invariance of ICs, provides fine-grained, spatially-aware feedback to enhance pattern accuracy.
- Extensive experiments demonstrate that LithoMamba significantly outperforms prior lithography simulation techniques as well as general-purpose generative models, in both quantitative metrics and qualitative fidelity.

II. Method

Our proposed LithoMamba framework uses a Mamba Generator with a global receptive field to synthesize the lithography process, which is adversarially trained against a fully convolutional Local Discriminator that provides fine-grained, spatially-aware feedback to preserve pattern fidelity.

This work was funded by the National Natural Science Foundation of China (Grants 62476092 and 62506131); the Natural Science Foundation of Shanghai (Grant 24JD1401300 and 25ZR1402126) and the China Postdoctoral Science Foundation (Grant 2025M771544 and GZC20240482).

978-3-9826741-1-7/DATE26/© 2026 EDAA

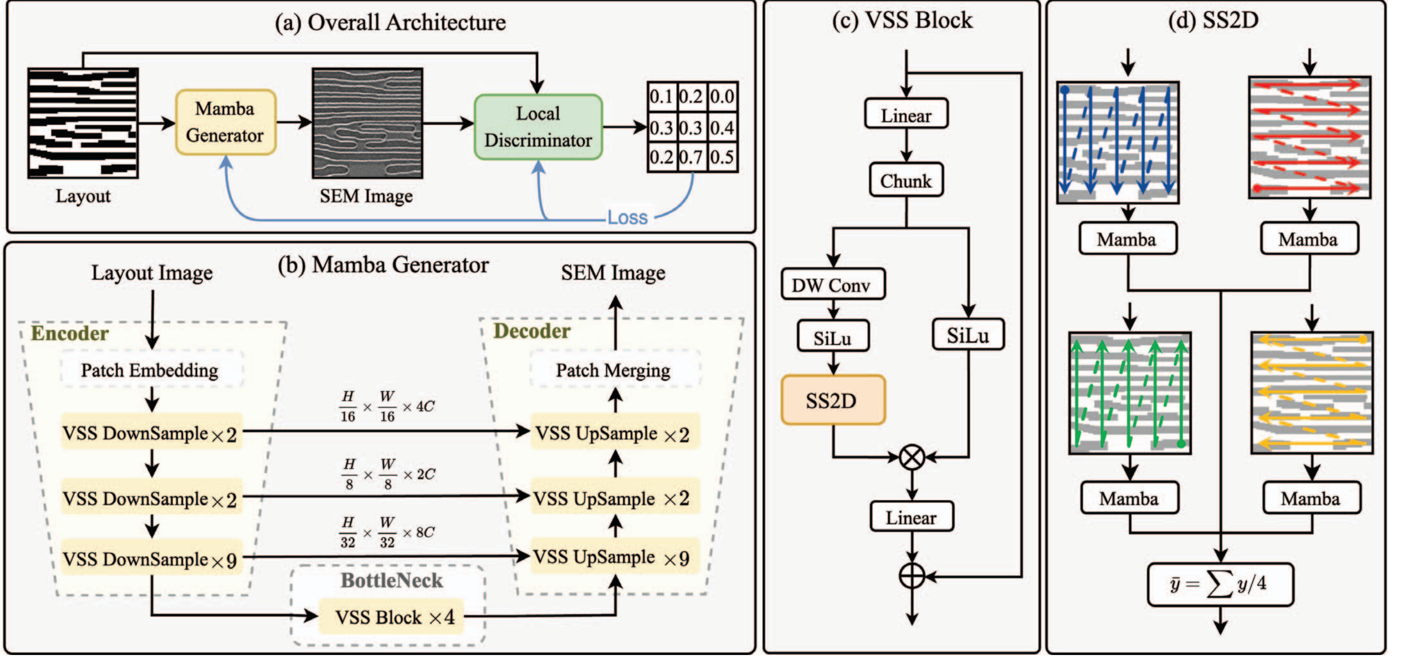

Fig. 1: The proposed LithoMamba lithography simulation network.

A. Mamba Generator

1) Generator Architecture: Our generator, depicted in Fig. 1(b), is designed as a hierarchical encoder-decoder network to transform an input IC layout into a photorealistic SEM image. The process begins with a *Patch Embedding* layer that converts the input layout image into patch-based features. The encoder then progressively downsamples the spatial resolution while increasing the feature dimensionality. Symmetrically, the decoder progressively restores the spatial resolution, ultimately reconstructing the final SEM image via *Patch Merging*. Crucially, the generator possesses a global receptive field at every level of the feature hierarchy. This is critical for modeling long-range physical phenomena in lithography, such as optical diffraction and proximity effects, which cannot be adequately captured by local operators like convolutions [16].

2) Visual Selective Scan Block (VSS Block): The VSS block, shown in Fig. 1(c), is the fundamental component of our generator. It has three parallel paths: a residual path, a gate path and a content path. By further adding a DownSample or UpSample module, it forms the encoder-decoder architecture. The final output is obtained by element-wise multiplication of the content path with gate path, followed by a linear projection and residual path. This structure allows the VSS block to dynamically select and fuse information based on global context dependencies.

3) Topology-Aligned Selective 2D-Scan (SS2D): To adapted the sequential Mamba model for 2D spatial data, we use topology-aligned scanning path to flattens the 2D feature map into four 1D sequences. The scanning strategy, as shown in Fig. 1(d) and Fig. 2, is specifically motivated by the topology priors of IC layouts, which predominantly composed of horizontal and vertical patterns. Aligning the scan directions with circuit structures enables Mamba to more effectively model dependencies along these critical paths. Each of the four sequences is processed by an independent Mamba model, and their outputs are subsequently averaged to produce the final output. The calculation of the state-space is written as

$$h_t = A(x)\, h_{t-1} + B(x)\, x, \tag{1}$$

$$y = C\, h_t + D\, x, \tag{2}$$

where h_t denotes the hidden state at time t, x is the input, y_t is the output, and $A(x)$, $B(x)$, C, and D are learnable parameter matrices. This process enriches the feature representation with contextual information from all four cardinal directions, enabling a comprehensive understanding of the 2D spatial relationships.

B. Local Discriminator

The Local Discriminator is designed to distinguish between real SEM images and those synthesized by our generator, conditioned on the input IC layout. To provide a stable and detailed training signal, we designed a fully convolutional, MLP-free discriminator. Our discriminator's architecture consists of a standard stack of convolutional layers for feature extraction followed by a sigmoid activation function. Critically, we remove the flattening and MLP layers that aggregate features into a single scalar output. Instead, the network outputs a 2D adversarial score map, where each element in the map corresponds to the realism of a specific receptive field in the SEM image.

This design is motivated by the strong translational invariance of IC patterns. By providing localized feedback, the discriminator forces the generator to focus on the fine-grained fidelity of local textures across the entire image. Comparing PatchGAN, our design allows overlays between receptive

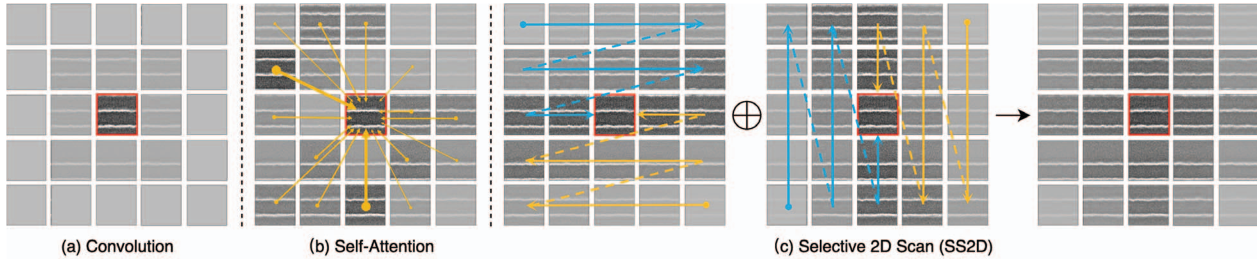

Fig. 2: Comparison of calculation between different model architecture.

fields and provides richer and more stable training signal. Furthermore, it guides our global Mamba Generator to render dexterous and physically accurate local patterns, ensuring both global consistency and local precision in the final synthesized image.

C. Loss Function

Our training objective is a composite loss function, combining an adversarial loss with an reconstruction loss to ensure both perceptual realism and structural fidelity, as in

$$L_{total} = L_{adv} + \lambda L_1. \quad (3)$$

The adversarial loss L_{adv}, derived from the 2D adversarial score map, provides spatially-aware training signals that guide the generator to refine local patterns across the synthesized image, while the complementary L_1 loss enforces pixel-level accuracy by minimizing absolute differences from the ground-truth SEM images. λ is a hyperparameter that balances two losses. Together, the localized adversarial feedback and direct structural guidance ensure both global physical consistency and local precision in the final results.

III. Experiments

A. Dataset

Due to the scarcity of public lithography simulation datasets, we constructed a new dataset from 14nm manufacturing nodes. It contains 3200 paired layout masks and their corresponding SEM images, captured at a 1024×1024 resolution and featuring diverse, complex IC patterns. We randomly split the data into training and testing sets using a 3:1 ratio.

B. Implementation Details

Our framework is implemented in PyTorch and was trained on the NVIDIA RTX 4090 GPU. We use the Adam optimizer [17] with hyper-parameters of $\beta_1 = 0.5$, $\beta_2 = 0.999$, and a learning rate of 2×10^{-4}. λ in the loss function is set to 0.1. All models are trained and evaluated at the original 1024×1024 resolution.

C. Baselines

We conduct a comprehensive comparison against a wide-range of methods, in three key categories: fully convolutional GANs such as PE-GAN [6] and SEM-GAN [7], recent methods that use the Fourier transform for global context modeling, like DAMO [11] and DOINN [12], and general synthesis models from the natural image domain, including a diffusion model, Palette [18], and ViT*, an adapted transformer-based GAN implementation that uses the ViT-UNet [19] as its generator.

TABLE I: Quantitative comparison of competing models for SEM image-level lithography simulation. Our LithoMamba achieves superior performance across all categories.

	IOU ↑	PA ↑	F1 ↑	FID ↓	PSNR ↑	SSIM ↑
SEM-GAN [7]	0.61	0.64	0.74	275.42	16.42	0.19
PE-GAN [6]	0.86	0.90	0.92	266.53	16.54	0.22
DAMO [11]	0.91	0.93	0.95	173.23	16.9	0.21
DOINN [12]	0.90	0.93	0.95	<u>89.71</u>	<u>16.93</u>	0.25
ViT* [19]	<u>0.92</u>	<u>0.94</u>	<u>0.95</u>	274.82	16.24	0.27
Palette [18]	0.86	0.88	0.91	97.87	16.73	<u>0.30</u>
Ours	**0.94**	**0.96**	**0.96**	**33.54**	**17.21**	**0.32**

D. Evaluation Metrics

We evaluate all methods from two perspectives: image fidelity and simulation accuracy. For **image fidelity**, we assess perceptual and structural quality using Fréchet Inception Distance (FID) [20], Peak Signal-to-Noise Ratio (PSNR), and Structural Similarity Index (SSIM) metrics. We evaluate **simulation accuracy** by comparing the simulated groove mask against the ground truth using Intersection over Union (IoU), Pixel Accuracy (PA), and the F1-Score. We employ UISS [21] on both simulated and real SEM images to obtain the groove masks. These scores quantify the structural similarity and indicate the potential performance in downstream applications [22].

E. Quantitative Comparison

As shown in Table I, our model, LithoMamba, demonstrates superior performance across all evaluation metrics. Those results also validate our central hypothesis: methods with a global receptive field (e.g., DAMO, DOINN, Transformer, and ours) consistently outperform localized, purely convolutional models (SEM-GAN, PE-GAN) in both simulation accuracy (IoU, PA, F1) and image fidelity.

Notably, our method achieves an FID score of **33.54**, drastically surpassing the next best model, DOINN (89.71). Our model surpass all competing methods in generating high-fidelity and structurally accurate simulations. These comprehensive results validate the effectiveness of the LithoMamba architecture for modeling complex, long-range lithography physics.

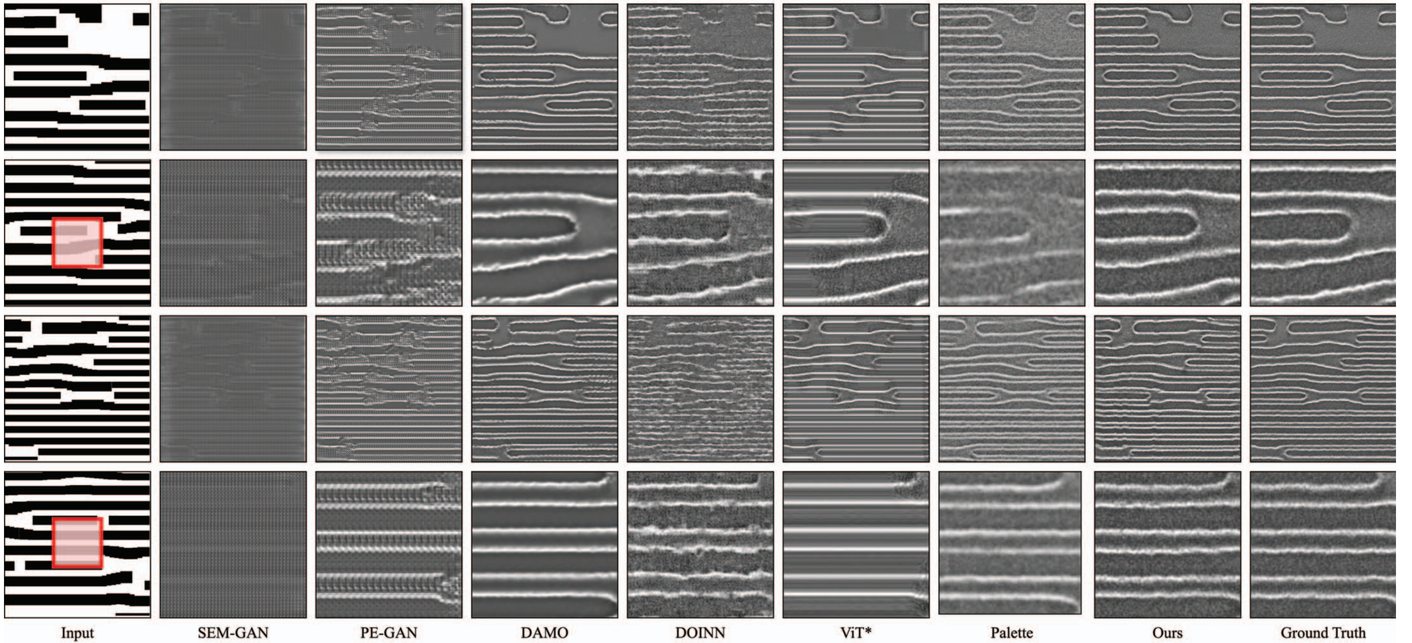

Fig. 3: Visual comparison of competing methods. Input are the layout image, Ground truth is the SEM image. Our proposed LithoMamba produces significantly more accurate simulation results under high resolution. Zoom in for best view.

F. Qualitative Comparison

The visual results in Fig. 3 underscore the superiority of our approach. The odd-numbered rows show magnified details, while the even-numbered rows display the full simulated results. Convolutional baselines (SEM-GAN, PE-GAN) fail to model the overall structure, producing distorted groove structures due to their limited receptive fields. While Fourier-based methods (DAMO, DOINN) capture global context better, they introduce distinct artifacts related to frequency, such as the loss of high-frequency details in DAMO and the structural fluctuation in DOINN.

Similarly, ViT* struggle to render the fine-grained, intricate groove geometries. Palette produces images with more detail but suffers from weak contrast and unnatural textures. This is because its diffusion process struggles to model the background SEM noise, which compromises simulation fidelity [23]. In contrast, our method faithfully reproduces realistic patterns that are visually almost indistinguishable from the ground truth, demonstrating superior simulation capability in both global and local visual fidelity.

G. Efficiency Analysis

To assess the computational efficiency of the proposed method, we analyze the throughput speed of all competing methods in Fig. 4. Our framework offers a compelling balance between performance and speed, crucial for practical deployment. While Fourier-based methods like DAMO are faster, they suffer from significant quality degradation due to the loss of high-frequency details. Conversely, LithoMamba is substantially more efficient than the computationally intensive Transformer and Diffusion models, demonstrating its suitability for high-throughput manufacturing environments.

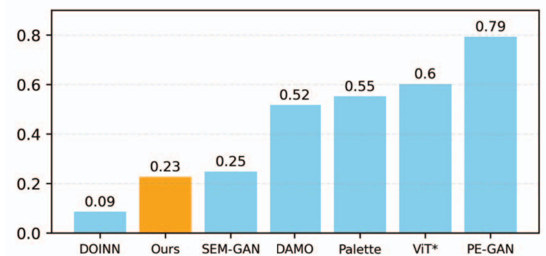

Fig. 4: Computation time per one image. Lower values means less computation resource needed and higher throughput.

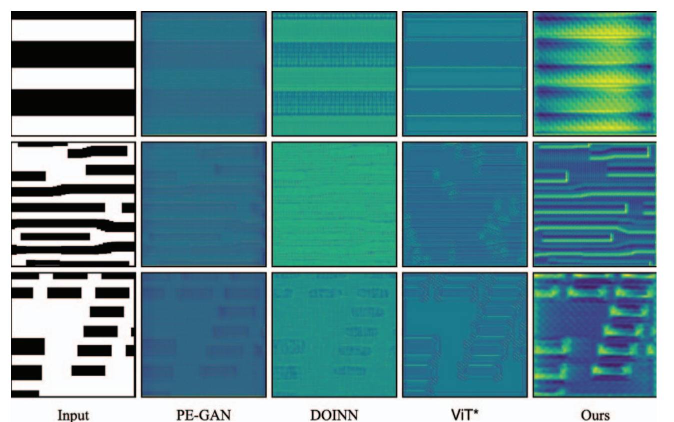

Fig. 5: Internal feature representations of LithoMamba. Unlike other methods that merely replicate the input layouts, our proposed LithoMamba generates feature maps that resemble the actual diffraction patterns in lithography physics.

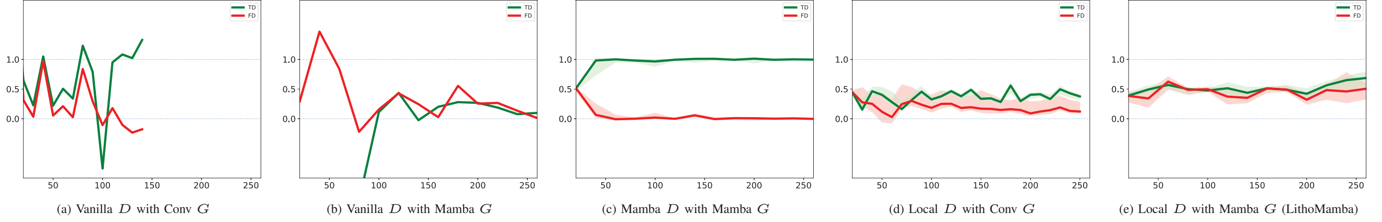

Fig. 6: Training stability of five different GAN configurations. The green line represents the mean output of the discriminator (D) for real images (TD), while the red line shows the output for generated images (FD). LithoMamba configuration (e) exhibits the most stable training dynamics.

TABLE II: Quantitative comparison of SEM image simulation across 32nm and 90nm technology nodes on the REFICS dataset.

Model	Node	IOU ↑	FID ↓	PSNR ↑	SSIM ↑
DOINN [12]	32nm	0.81	208.55	16.71	0.36
ViT* [19]		0.82	49.95	17.18	0.37
Ours		**0.84**	**41.60**	**18.62**	**0.37**
DOINN [12]	90nm	0.74	134.25	16.22	0.32
ViT* [19]		0.77	49.46	16.83	0.33
Ours		**0.78**	**47.37**	**17.04**	**0.34**

TABLE III: Ablation study on the generator architecture. ”-” means vanilla implementation.

G	D	IOU ↑	PA ↑	F1 ↑	FID ↓	PSNR ↑	SSIM ↑
-	-	0.74	0.79	0.81	213.71	15.71	0.16
-	Local	0.84	0.82	0.87	166.53	16.08	0.18
Mamba	-	0.90	0.93	0.95	84.18	16.36	0.21
Mamba-Inward	Local	0.83	0.88	0.91	124.91	15.45	0.17
Mamba-diagonal	Local	0.88	0.91	0.93	53.31	15.98	0.19
Transformer	Local	0.92	0.94	0.95	274.82	16.24	0.27
Ours		**0.94**	**0.96**	**0.96**	**33.54**	**17.21**	**0.32**

H. Analysis of Internal Feature Representation

To investigate the architectural advantages of our model, we visualized the penultimate feature maps of competing methods in Fig. 5. The feature maps from purely convolution method (PE-GAN) shows limited generative capability with only rectangular motifs. DOINN and ViT* show improved details but the overall patterns lack explicit representations of the physical optic interaction in lithography.

In contrast, the feature maps generated by our LithoMamba are more detailed and resemble the coherent patterns of optical diffraction after light passes through the layout mask. This interesting finding suggests our model learns a more physically meaningful representation of the lithography process, providing a possible explanation for its state-of-the-art simulation accuracy.

I. Evaluation on Public 32nm and 90nm Datasets

To validate the effectiveness and generalization of our model, we conduct a quantitative comparison on the 32nm and 90nm technology nodes from the REFICS [24] dataset. All models were trained from scratch with the same hyper-parameter settings. As shown in Table II, LithoMamba consistently outperforms competing methods in both nodes, with a notable advantage in FID scores. These results validate the effectiveness and robustness of our proposed approach for high-fidelity SEM image simulation across different technology nodes.

J. Ablation Study

1) Validation of the Architecture: We validate our key architectural choices in Table III. The results clearly demonstrate that both the Mamba Generator and the Local Discriminator are critical components. Replacing either with a vanilla counterpart causes a significant drop in performance, representing that the full design is optimal to achieve stable and high-fidelity SEM image simulation.

Furthermore, we confirm the effectiveness of our topology-aligned 2D scanning mechanism. It markedly outperforms alternative scanning paths (spin-inward and 45 degree diagonal scan) and a standard Transformer block, validating our design choice to align the scanning process with the inherent structural priors of IC layouts.

2) Ablation on the Convergence of Architectural Compositions: To analyze training stability, we visualize the discriminator outputs in Fig. 6. Our proposed framework (e) achieves a stable training equilibrium, where the discriminator outputs for real and fake samples remain balanced around the ideal 0.5 threshold. In contrast, other generator-discriminator pairings exhibit unstable dynamics, such as rapid discriminator convergence (c), which leads to vanishing gradients and prevents the generator from learning effectively. This confirms that our global-local architecture not only improves final performance but also fosters a more stable and effective adversarial training process.

IV. CONCLUSION

In this paper, we introduced LithoMamba, the first network to successfully leverage a State Space Model (Mamba) for high-fidelity lithography simulation. Our novel architecture combines a global Mamba Generator, which excels at modeling long-range optical physics, with a local convolutional discriminator that enforces fine-grained pattern accuracy. Extensive experiments show that our method sets a new state-of-the-art, significantly outperforming previous techniques in both quantitative metrics and visual quality. This work highlights the immense potential of SSMs for computational lithography and opens new avenues for physics-aware generative modeling in semiconductor manufacturing.

REFERENCES

[1] Su Zheng, Haoyu Yang, Binwu Zhu, Bei Yu, and Martin D.F. Wong, "Lithobench: benchmarking ai computational lithography for semiconductor manufacturing," in *Proceedings of the 37th International Conference on Neural Information Processing Systems*, Red Hook, NY, USA, 2023, NIPS '23, Curran Associates Inc.

[2] Guojin Chen, Ziyang Yu, Hongduo Liu, Yuzhe Ma, and Bei Yu, "Develset: Deep neural level set for instant mask optimization," *IEEE Transactions on Computer-Aided Design of Integrated Circuits and Systems*, vol. 42, no. 12, pp. 5020–5033, 2023.

[3] Wei Ye, Mohamed Baker Alawieh, Yibo Lin, and David Z Pan, "Lithogan: End-to-end lithography modeling with generative adversarial networks," in *Proceedings of the 56th Annual Design Automation Conference 2019*, 2019, pp. 1–6.

[4] Haoyu Yang, Zongyi Li, Kumara Sastry, Saumyadip Mukhopadhyay, Mark Kilgard, Anima Anandkumar, Brucek Khailany, Vivek Singh, and Haoxing Ren, "Generic lithography modeling with dual-band optics-inspired neural networks," in *Proceedings of the 59th ACM/IEEE Design Automation Conference*, 2022, pp. 973–978.

[5] Haoyu Yang and Haoxing Ren, "Enabling scalable ai computational lithography with physics-inspired models," in *2023 28th Asia and South Pacific Design Automation Conference (ASP-DAC)*, 2023, pp. 715–720.

[6] He Xinyu, Daohui Wang, Wenzhan Zhou, Kan Zhou, Xintong Zhao, Shujing Lyu, Jiwei Shen, and Yue Lu, "Photolithographic image prediction with conditional adversarial network and parameter encoding," in *Eighth International Workshop on Advanced Patterning Solutions (IWAPS 2024)*, Yayi Wei and Tianchun Ye, Eds. International Society for Optics and Photonics, 2024, vol. 13423, p. 134230O, SPIE.

[7] Botong Zhao, Jiwei Shen, Hu Lu, Pengjie Lou, Wenzhan Zhou, Kan Zhou, Xintong Zhao, Shujing Lyu, and Yue Lu, "Pix2pixhd-based generation of sem image in the etch domain by sem image of litho domain," in *2023 International Workshop on Advanced Patterning Solutions (IWAPS)*, 2023, pp. 1–3.

[8] Kevin D Lucas, Hiroyoshi Tanabe, and Andrzej J Strojwas, "Efficient and rigorous three-dimensional model for optical lithography simulation," *JOSA A*, vol. 13, no. 11, pp. 2187–2199, 1996.

[9] T. A. Brunner, "Impact of lens aberrations on optical lithography," *IBM Journal of Research and Development*, vol. 41, no. 1.2, pp. 57–67, 1997.

[10] Benjamin D. Bunday, Michael Bishop, Donald W. McCormack Jr., John S. Villarrubia, Andras E. Vladar, Ronald Dixson, Theodore V. Vorburger, N. George Orji, and John A. Allgair, "Determination of optimal parameters for CD-SEM measurement of line-edge roughness," in *Metrology, Inspection, and Process Control for Microlithography XVIII*, Richard M. Silver, Ed. International Society for Optics and Photonics, 2004, vol. 5375, pp. 515 – 533, SPIE.

[11] Guojin Chen, Wanli Chen, Qi Sun, Yuzhe Ma, Haoyu Yang, and Bei Yu, "Damo: Deep agile mask optimization for full-chip scale," *IEEE Transactions on Computer-Aided Design of Integrated Circuits and Systems*, vol. 41, no. 9, pp. 3118–3131, 2022.

[12] Guojin Chen, Zehua Pei, Haoyu Yang, Yuzhe Ma, Bei Yu, and Martin D. F. Wong, "Physics-informed optical kernel regression using complex-valued neural fields," *arXiv*, 2023.

[13] Albert Gu and Tri Dao, "Mamba: Linear-time sequence modeling with selective state spaces," *arXiv preprint arXiv:2312.00752*, 2023.

[14] Jiarun Liu, Hao Yang, Hong-Yu Zhou, Yan Xi, Lequan Yu, Yizhou Yu, Yong Liang, Guangming Shi, Shaoting Zhang, Hairong Zheng, and Shanshan Wang, "Swin-umamba: Mamba-based unet with imagenet-based pretraining," *arXiv*, 2024.

[15] Haoyang He, Yuhu Bai, Jiangning Zhang, Qingdong He, Hongxu Chen, Zhenye Gan, Chengjie Wang, Xiangtai Li, Guanzhong Tian, and Lei Xie, "Mambaad: Exploring state space models for multi-class unsupervised anomaly detection," *arXiv preprint arXiv:2404.06564*, 2024.

[16] Ziyang Wang, Jian-Qing Zheng, Yichi Zhang, Ge Cui, and Lei Li, "Mamba-unet: Unet-like pure visual mamba for medical image segmentation," *arXiv*, 2024.

[17] Diederik P. Kingma and Jimmy Ba, "Adam: A method for stochastic optimization," *arXiv*, 2017.

[18] Chitwan Saharia, William Chan, Huiwen Chang, Chris Lee, Jonathan Ho, Tim Salimans, David Fleet, and Mohammad Norouzi, "Palette: Image-to-image diffusion models," in *ACM SIGGRAPH 2022 Conference Proceedings*, New York, NY, USA, 2022, SIGGRAPH '22, Association for Computing Machinery.

[19] Nan Zhou, Mingming Xu, Biaoqun Shen, Ke Hou, Shanwei Liu, Hui Sheng, Yanfen Liu, and Jianhua Wan, "Vit-unet: A vision transformer based unet model for coastal wetland classification based on high spatial resolution imagery," *IEEE Journal of Selected Topics in Applied Earth Observations and Remote Sensing*, vol. 17, pp. 19575–19587, 2024.

[20] Martin Heusel, Hubert Ramsauer, Thomas Unterthiner, Bernhard Nessler, and Sepp Hochreiter, "Gans trained by a two time-scale update rule converge to a local nash equilibrium," in *Advances in Neural Information Processing Systems*, I. Guyon, U. Von Luxburg, S. Bengio, H. Wallach, R. Fergus, S. Vishwanathan, and R. Garnett, Eds. 2017, vol. 30, Curran Associates, Inc.

[21] Nils Rothaug, Simon Klix, Nicole Auth, Sinan Böcker, Endres Puschner, Steffen Becker, and Christof Paar, "Towards unsupervised sem image segmentation for ic layout extraction," in *Proceedings of the 2023 Workshop on Attacks and Solutions in Hardware Security*, New York, NY, USA, 2023, ASHES '23, p. 123–128, Association for Computing Machinery.

[22] Zhikun Wang, Pengfei Lin, Phuc Nguyen, Jingyan Wang, and ChaBum Lee, "Line-edge-roughness characterization of photomask patterns and lithography-printed patterns," *Precision Engineering*, vol. 88, pp. 235–240, 2024.

[23] M Satya Prasad and David C Joy, "Is sem noise gaussian?," *Microscopy and Microanalysis*, vol. 9, no. S02, pp. 982–983, 07 2003.

[24] Ronald Wilson, Hangwei Lu, Mengdi Zhu, Domenic Forte, and Damon L. Woodard, "Refics: Assimilating data-driven paradigms into reverse engineering and hardware assurance on integrated circuits," *IEEE Access*, vol. 9, pp. 131955–131976, 2021.